Reflectance and thermoreflectance spectra of CuI and CuBr

P. D. Martzen and W. C. Walker
Department of Physics, University of California, Santa Barbara, California 93106
(Received 9 July 1979)

The results of an experimental study of the interband transitions of the cuprous halides, CuI and CuBr, are reported. High-resolution, low-temperature, near-normal incidence reflectance and thermal modulated reflectance spectra were studied over the range 3–10 eV. Thin-film samples, prepared by vacuum deposition, and a single-crystal sample of CuI were measured. Spectral structures are assigned to specific interband transitions in the Brillouin zone on the basis of splittings and temperature shifts, and compared with the predictions of the Phillips–Van Vechten ionicity theory of energy-gap trends in zinc-blende-structured isoelectronic sequences.

INTRODUCTION

The cuprous halides occupy an important position among the zinc-blende semiconductors, since they form the end point of several isoelectronic sequences.

A general theory of trends in the electronic structure of such sequences has been developed by Phillips[1] and Van Vechten.[2] Based on a few simple parameters such as the dielectric constant, the lattice constant, and the electronic structure of silicon, Phillips and Van Vechten have made predictions for the interband energy gaps of the cuprous halides. It would thus be desirable to have accurate measurements of interband energies to check these predictions.

Previous optical studies of the cuprous halides date back to 1931 with absorption measurements[3] on CuCl to 1600 Å and in 1937 to the LiF cutoff.[4] In 1960 Herman and McClure[5] interpreted the absorption spectra of the cuprous halides. They suggested that there were two valence bands with the top band being of $3d$ Cu character and the second being of halide p character. They also noted a lack of correlation with other compounds of the isoelectronic sequences. More detailed absorption and reflectance measurements were obtained by Cardona[6] in 1963. Cardona noted that the reflectance spectra of the three halides exhibit three distinct maxima, except in the case of CuCl where the first two maxima coincide. He labeled these peaks E_1, E_0', and E_2, for the first, second, and third reflectance maxima. The low-energy peak at 4.6 and 5.3 eV in CuI and CuBr was assigned to transitions at the L point from the top valence band to the first conduction band. The second series of peaks at 6.0, 6.3, and 6.1 eV for CuI, CuBr, and CuCl, respectively, were attributed to transitions from the top valence band to the second conduction band at $k=0$ on the basis of the observed splitting. The highest observed peaks at 8.0, 8.9, and 8.3 eV were usually doublets with splittings comparable to that expected between the first and second conduction bands at the X point and were assigned accordingly. The spin-orbit splitting of the two excitons at $k=0$ was measured and used to estimate the ratio of p-d character in the upper valence band of the three halides. In 1965 Shindo[7] verified Cardona's interpretation concerning the spin-orbit splitting and showed in particular that the copper d bands gave a negative contribution.

In 1967 the first band calculation of CuCl was obtained by Song[8] using tight-binding and orthogonalized-plane-wave methods for the valence and conduction bands, respectively. The calculations showed two valence bands as suggested previously, with the lower valence band corresponding to the usual top valence band for other zinc-blende compounds. The average splitting between the two valence bands was about 3 eV. Band-structure diagrams for CuBr and CuI were extrapolated from that calculated for CuCl on the basis of a perturbation scheme, due to Herman,[9] in which the interband transition energies essentially scale as the valence difference squared. Based upon his calculations, Song reinterpreted the reflectance spectra assigning the E_1 and E_0' peaks to transitions from the second valence band to the first conduction band at $k=0(\Gamma_{15}^{v2}-\Gamma_1^{c1})$ and to $L_3^{v1}-L_1^{c2}$, respectively.

In 1971 soft x-ray absorption spectra[10] of the CuCl Cl^- $2p$-to-conduction-band transitions were obtained. These spectra showed four pairs of absorption maxima attributed to excitons. These results did not agree with Song's band calculations.

Fundamental ultraviolet-absorption spectra[11] of CuCl and CuBr above 3 eV were reported in 1972 and compared to the Cl^- $2p$ absorption. The absorption maxima near 6.5 eV was attributed to transitions from the second p-like valence band to the first conduction band in agreement with

Song's interpretation.

The first direct evidence of two valence bands for the cuprous halides was obtained by photoemission measurements.[12-15] Kono *et al.*[13] were able to estimate the ratio of the average p-d mixing of the top valence bands. Values obtained were not consistent with earlier results in which the top valence band is dominated by d-character electrons and the lower valence band by p-character electrons. Kono *et al.* attributed these peaks to transitions from the top of the lower valence band to the bottom of the first conduction bands $\Gamma_{15}^{v_2}$-$\Gamma_1^{c_1}$. They also suggest that the p character of states near X_3 of the first conduction band may be significant so that transitions from the d-like region of the top valence band near the X point may be significant. Accordingly the E_1 peak was assigned to this region.

In later ultraviolet-photoemission experiments Goldmann *et al.*[14] obtained partial densities of valence states and estimated the p-d mixing at $k=0$ in the top valence band. The results were in good agreement with those obtained by Cardona from the spin-orbit splitting of the fundamental exciton spectra.

Orthogonalized-plane-wave conduction-band calculations of CuCl by Song were extended in 1972 by Khan.[16,17] This calculation gave reasonable results when compared to the Cl^- $2p$ absorption data obtained by Sato *et al.*[15] The E_1 and E_0' peaks in the ultraviolet absorption were attributed to transitions between two of the double-group representations of the top valence band and the first conduction band at the X point. This assignment was made on the basis of the observed splitting since the calculated transition energy was 1 eV less than experimental values. The peaks designated E_2 and E_2' were also assigned to transitions at the X point.

The valence and conduction bands were also calculated by Calabese and Fowler[18] at about the same time using a combined plane-wave tight-binding "mixed-bases" method. The separation between the two top valence bands was calculated to be about 1.7 eV larger than that calculated by Song, thus giving better agreement with photoemission data. One interesting feature of this calculation is that there is no apparent splitting between X_3 and X_1 of the first and second conduction bands. This is contrary to accepted models in which this splitting increases as a function of ionicity.[2]

In 1973 Khan[19] calculated the band structure of CuBr using the orthogonalized-plane-wave method for the conduction bands and a tight-binding method up to the sixth-nearest neighbor for the valence bands. The calculated conduction bands were quite similar to those calculated for CuCl. However, the Γ_{15} point of the lower p-like valence band is a minima with a 15-eV separation from Γ_{15} of the top valence band. This is in contrast to CuCl, where Γ_{15} of the second valence band is a maximum according to all previous calculations. Khan attributed the prominent ultraviolet-absorption structure to transitions at the X point as done previously for CuCl.

Recent work[20] suggests that temperature effects on photoemission may be used to study orbital hybridization of solids with certain ranges of Phillip's ionicities. Following these suggestions, Lin *et al.*[21] obtained photoemission spectra of CuBr at photon energies between 8.0 and 11.8 eV at 77 and 295 K, respectively. Analysis of the temperature dependence of the electron density-of-states curves provided further evidence that a pure d band exists between the two valence bands and that the top valence band has a mixed p-d character.

In 1977 room-temperature reflectance measurements of cleaved single crystals up to 30 eV were reported by Lewonczuk *et al.*[22] The experimental reflectance spectra agree with previous measurements except for the E_0' peak which appears at 6.1 eV in Cardona's spectra and at 5.4 eV in the spectra of Lewonczuk *et al.* They assigned the E_0' and E_2' peaks to transitions at the X point similar to Khan's assignments.

In a subsequent paper[23] by the same group the valence-band structure of CuI, calculated by a tight-binding method, is reported and shows the same behavior as CuBr. Deformation-potential[24] measurements of the $Z_{1,2}, Z_3$ excitons and the E_1 peak suggest that the two valence bands are considerably more mixed in CuI than in CuCl or CuBr.

A self-consistent first-principles band-structure calculation has been performed for CuCl by Zunger and Cohen.[25] These authors point out that agreement with experiment is generally very good except for the value of the fundamental gap which is too low by 40%. The results, however, were not compared with the recent experimental reflectance spectra of Lewonczuk *et al.*[22]

Recent optical studies by the authors[26] and by Gross *et al.*[27] have revealed new fine structure in the reflectance and thermoreflectance spectra of CuI and CuBr at low temperatures.

EXPERIMENTAL METHODS

In the present study the electronic structure of the cuprous halides was studied using reflectance and thermoreflectance techniques.

Reflectance

The reflectance $R=I_R/I_0$ can be related to the real and imaginary parts of the dielectric function

by Fresnel's equation and the Kramers-Kronig relation by standard expressions. Usually at frequencies well above the fundamental absorption edge, reflectance structure is similar to that of ϵ_2, and little error is introduced by assigning structure directly from reflectance data.

Thermoreflectance

The thermoreflectance technique is described in detail by Cardona[28] and Batz.[29] Briefly, the sample reflectance is modulated periodically by heat pulses and the quantity $(1/R)dR/dT$ measured by dividing the ac by the dc component of the photomultiplier output. Detailed line shapes are complex and involve changes in both interband gap and broadening parameters.

The modulated reflectance phase angle can be obtained from $\Delta R/R$ by a Kramers-Kronig integral

$$\Delta\theta(\omega)=\frac{\omega}{\pi}\int_0^\infty \frac{(\Delta R/R)(\omega')-(\Delta R/R)(\omega)}{\omega'^2-\omega^2}\,d\omega'.$$

In the present study this integration was performed by a computer with $\Delta R/R=0$ outside the region of interest. For $\omega=\omega'$ the value of the integrand was obtained by interpolation from neighboring points. The $\Delta\epsilon_1$ and $\Delta\epsilon_2$ were then obtained from

$$\Delta\epsilon_1=\tfrac{1}{2}n(n^2-1-k^2)\Delta R/R+k(3n^2-1-k^2)\Delta\theta\,,$$

$$\Delta\epsilon_2=\tfrac{1}{2}k(3n^2-1-k^2)\Delta R/R+n(3k^2+1-n^2)\Delta\theta\,,$$

where n and k are the real and imaginary parts of the refractive index of the sample, respectively.

The optical constants were obtained from a Kramers-Kronig analysis of our data using a method devised by Roessler.[30]

PHILLIPS-VAN VECHTEN THEORY

Phillips and Van Vechten[1,2] have proposed an isotropic two-band model of covalent solids with which they can account for systematic trends in energy gaps and dielectric properties. They assume that the complex potential for the smallest reciprocal lattice vector can be used to represent an average energy gap E_g given by

$$|E_g|^2=E_h^2+C^2,$$

where E_h is the symmetric or homopolar part and C is the antisymmetric or ionic contribution. By assuming that E_h scales with d, the nearest-neighbor separation, and using silicon as a standard, they deduce for zinc-blende-structured (ZB) materials AB the relation

$$E_h(AB)=E_h(\mathrm{Si})\left(\frac{d(AB)}{d(\mathrm{Si})}\right)^{-s},$$

where $s=2.48$. Extending this relation to include all members of the isoelectronic sequence, they were able to make predictions for the energy gaps of a large class of ZB materials. To date their predictions at large ionicity or large C have not been adequately tested. The interpretation of optical data for CuI and CuBr presented below provides such a test.

APPARATUS

Optical system

Reflectance spectra were obtained with a system employing a dc hydrogen discharge operating at 350 mA, a McPherson 225, 1-m normal-incidence monochromator with a 600-line/mm grating blazed at 1600 Å and a high-vacuum, low-temperature reflectometer with a LiF window. The monochromator exit beam was focused by a toroidal mirror to a 2×0.2-mm^2 area on the sample at an incidence angle of 22°.

The reflected intensity was directed by a second plane mirror onto a sodium-salicylate-coated quartz window and detected by a Centronic Q4283RA photomultiplier operated at room temperature. The reflectometer was also equipped with a quartz filter which could be rotated into the incident beam for measurements above 2100 Å. A third small Al mirror overcoated with MgF_2 was mounted on the cold finger above the sample and was used to normalize the reflectance spectra.

The reflectometer consisted of a stainless steel $12\times12\times6$-in.^{3} chamber connected to the exit slit of the monochromator by a 10-in.-long × 6-in.-diam tube. The sample was mounted on the cold finger of a Janis liquid-helium Dewar which passed through the top of the reflectometer by means of bellows and could be raised or lowered to align the sample with the incident light beam.

The pumping system for the reflectometer consisted of a Varian 80-l/s Vacion pump and a Varian Vacsorb roughing pump. The Vacion pump was able to attain a pressure of 4×10^{-8} Torr when the outer Dewar jacket was cooled with liquid nitrogen. A LiF window separated the oil-diffusion pumped vacuum of the monochromator from that of the ion-pumped reflectometer and limited measurements to photon energies below 11.5 eV.

Electronics

The output of the photomultiplier was amplified by a PAR 122 photometric preamplifier, and used to control a PAR 280 photomultiplier high-voltage supply to maintain a fixed photomultiplier-tube current. The preamplifier provided separate ac and dc outputs. The ac component was provided by a high-pass 6-dB/octave filter (6-dB point at

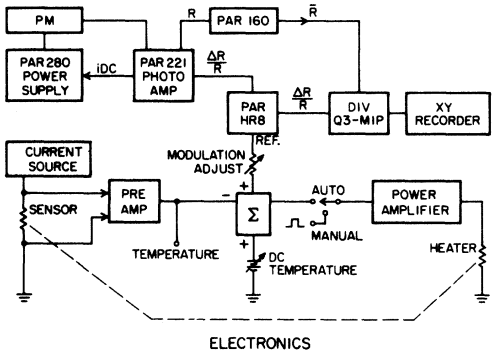

FIG. 1. Schematic diagram of the electronics used for the thermoreflectance measurements.

1 Hz). The rms value of the ac modulation signal was synchronously detected by a PAR HR8 lock-in amplifier and applied to the numerator input of a Philbrick analog divider. The dc component was further amplified and filtered by a PAR 160 Boxcar amplifier operated in continuous mode and applied to the denominator input of the divider. The $\Delta R/R$ signal was obtained from the output of the divider and plotted on an xy chart recorder as shown in Fig. 1.

Temperature modulation

Temperature modulation was obtained by applying current pulses through a thin-film heater next to the cuprous halide film on a sapphire substrate. The substrate was clamped to a copper cold finger with silicon grease which provided the necessary thermal contact.

The temperature-modulation system consisted of heater and temperature sensor films on the substrate and a temperature controller. A 120-Å-thick by 4- × 2-mm Cu film was used for the sample heater. A 1.6-μm-thick by 60-μm-wide by 4-mm-long lead film deposited near one edge of the heater was used for the temperature sensor. A platinum resistor on the rear of the cold finger was used for calibration of the lead temperature sensor.

Electrical insulation between the heater and temperature sensor films was provided by a 2000-Å evaporated layer of SiO. SiO was also evaporated as the final film between the temperature sensor and the cuprous halide to prevent any reaction between the halide and the lead film.

Thick (2-μm) Cu films, two for the temperature sensor film and two for the heater film, were evaporated near the edge of the substrate and used for electrical contact points. It was found that the maximum allowable current through the heater was determined by the contact resistance between the heater spring contacts and the thick Cu pads, and was limited to about 2 A.

Sample preparation

Cuprous halide films were evaporated using an Edwards vacuum system with a 14-in.-diam bell jar, pumped by a 4-in.-liquid-N_2 trapped oil diffusion pump. The system could obtain a base pressure of better than 10^{-6} Torr after a mild bake-out to approximately 80°C.

The typical procedure was to prepare 3–4 substrates with the temperature sensor and heater. The substrates were stored in a desiccator until needed. Then the apparatus for the cuprous halide deposition was installed, and the system was baked-out for 4 h without the evaporant and substrate. With the surfaces still hot the cuprous halide evaporant and substrate were installed and the system evacuated again with a second mild bake-out. The copper halide sample was evaporated after the base pressure returned to 10^{-6} Torr. The sample was placed in an argon-purged dessicator until it could be mounted on the cold finger. The samples were normally exposed to the atmosphere for about 2 min.

Single-crystal samples were polished with a slurry of ethylene glycol and 0.3-μm alumina on a Politex-D mat. Etching was accomplished with a 10% solution of HNO_3. The completed single-crystal samples were about 0.5 mm thick.

Data-acquisition system

Data acquisition and analysis was done with an on-line PDP-15 computer.

The system consisted of (1) real-time normalization of reflectance data, (2) digitizing of thermo-reflectance data, and (3) data plotting on a 12-in. Calcomp plotter. Two methods of data acquisition were utilized, one suitable for on-line data acquisition or digitizing chart-recorder plots and the second for digitizing xy-recorder plots. The arrangement is shown in Fig. 2, which indi-

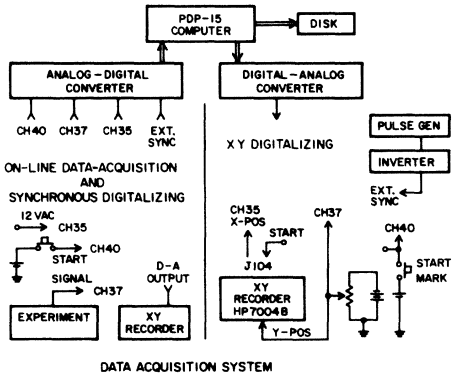

FIG. 2. Schematic diagram of the data-acquisition system.

cates schematically the PDP-15 computer and two methods of transferring data to the computer.

The data-acquisition system used a 13-bit, 64-channel analog-to-digital (AD) converter for data input and a 10-bit, digital-to-analog (DA) converter as a data monitor. A Dec-writer terminal controlled the computer from the laboratory and was used to input program parameters such as photomultiplier gain, the number of conversions per second, and the total number of conversions. Since the monochromator utilized a synchronous motor for the wavelength drive, the computer and experiment were synchronized by having the computer monitor the 60-Hz power and perform AD conversions at multiples of 1/60 s. This system gave good synchronization at monochromator scanning rates of 200 Å/min with the slits set for 5-Å resolution. A monitor line from the DA converter was programmed to send a time-varying voltage representing either the instantaneous AD input or a ratio back to the experimental site. The ratio mode was used to obtain real-time plots of sample reflectance on an *xy* recorder in the lab.

RESULTS

Near-normal incidence reflectance and thermoreflectance data on thin polycrystalline cuprous halide films were taken over the range 3.1–10 eV (4000–1200 Å) between room temperature and liquid-nitrogen temperature. Reflectance and thermo-reflectance measurements were also taken on a CuI single-crystal sample obtained from Dr. D. Biegelson of Xerox Research Center, Palo Alto, California.[31]

Thin-film samples were evaporated without further preparation from powder obtained from Apache Chemicals.[32] The stated purity values were 99.99% for CuI, 99.999% for CuBr, and 99.999% for CuCl.

In general the reflectance of the best thin-film samples below 7.5 eV was similar to previous measurements.[6,22] Above 7.5 eV the absolute reflectance of some films was lower than that of other workers, although in later samples this was improved somewhat. The positions of reflectance maxima, however, agreed with previous results throughout the entire energy range studied. Even though the reflectometer pressure was only a few times, 10^{-8} Torr, and a cold shield was used, a considerable decrease in the sample reflectance was often observed after 10 h of measurements at liquid-nitrogen temperature.

CuI reflectance

The reflectance spectrum of a CuI single-crystal sample taken at 77 K, with 5-Å resolution is shown in Fig. 3. The gross features are three major peaks at 4.68, 6.00, and 8.04 eV. These peaks were also observed in thin-film samples and by other workers. In addition, shoulders and small peaks at 5.0, 6.2, 6.5, 7.3, 7.7, and 8.8 eV were more clearly resolved than in previous work.[22] The small peak at 3.7 eV is the Z_3 exciton.[6] For the three major peaks we obtained reflectance values of 20.5%, 24.5%, and 22.4% compared to 21.2%, 22.1%, and 19.6% observed by Cardona[6] and 20.0%, 24.3%, and 29.9% observed by Lewonczuk *et al.*[22]

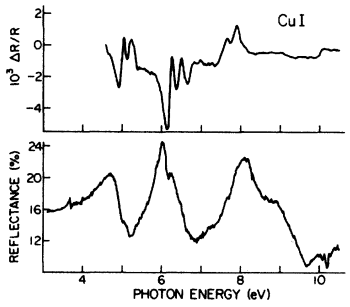

FIG. 3. Reflectance R at 77 K and thermoreflectance $\Delta R/R$ at 88 K, of a single crystal of CuI.

A Kramers-Kronig analysis of the CuI reflectance was performed using Roessler's method.[30] The results are shown in Fig. 4.

CuI thermoreflectance

The thermoreflectance (TR) spectrum of a single-crystal sample taken at 88 K, with 5-Å resolution is also shown in Fig. 3. The sample temperature modulation was 13 K peak to peak at a frequency of 2 Hz.

Beginning with the region of the first reflectance maxima at 4.68 eV there are two minima in the TR spectra which correspond to the maxima at 4.68 and the shoulder at 5.00 eV in the reflectance.

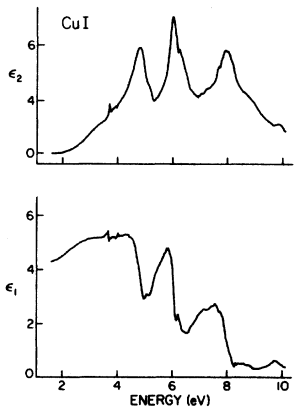

FIG. 4. Dielectric functions $\epsilon_1(\omega)$ and $\epsilon_2(\omega)$ for CuI.

At 5.39 eV there is a small dip which corresponds to a small shoulder near the bottom of the second reflectance peak. Between 6.10 and 6.62 eV there are three TR minima which we associate with the reflectance maxima at 6.0 eV and less noticeable structure on the high-energy side of that peak. On the third reflectance maxima one notices a shoulder at 7.30 eV which could be associated with a slight TR minima at 7.36 eV. TR maxima at 7.64 and 7.90 eV are associated with the reflectance shoulder and peak at 7.65 and 8.04 eV. Finally, there is a shoulder at 8.8 eV in the reflectance and a broad TR maxima near that energy. There appears to be additional TR structure above 9.0 eV but because of excessive noise its significance is in doubt. TR spectra of thin-film samples generally exhibited similar structure.

CuBr reflectance

The reflectance spectrum of a CuBr thin-film sample taken at 77 K with 5-Å resolution is shown in Fig. 5. The principal peaks located at 5.2, 6.4, 7.7, and 9.0 eV were also observed by other workers. Lewonczuk *et al.*[22] reported peaks at 5.07, 6.3, 7.8, and 9.0 eV. Cardona reported peaks at 5.3, 6.3, 7.3, and 8.9 eV. The relative peak heights of the room-temperature reflectance spectrum agree with previous results. However, the low-temperature results shown here exhibit a sharp decrease near 7.8 eV. The same feature appears in the 77-K reflectance spectrum of a single-crystal sample of CuBr. An additional feature not observed in the room-temperature reflectance is the shoulder at 7.3 eV.

CuBr thermoreflectance

The thermoreflectance spectrum of CuBr near 85 K with 15-Å resolution is also shown in Fig. 5. An average square-wave modulation of 0.8 W at 7 Hz (estimated 10 K peak to peak) was applied to the sample.

Four major minima occur at 6.6, 7.3, 7.8, and 9.0 eV, which can be associated with structure in the reflectance spectrum.

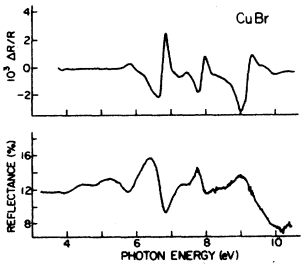

FIG. 5. Reflectance R at 77 K and thermoreflectance $\Delta R/R$ at 85 K, of a thin film of CuBr.

The TR structure near 5.8 eV may be associated with the reflectance peak at 5.2 eV, but there is no TR structure corresponding to the reflectance peak at 4.4 eV.

DISCUSSION

CuI

The positions of prominent structure in CuI are summarized in Table I, and indicated on the ionicity plot for the Ge-Sn, InAs, ZnTe, and CuI isoelectronic sequence in Fig. 6.

The thermo-reflectance spectrum shows at least two distinct minima in the region of the first peak, one of which coincides with the reflectance shoulder at 5.04 eV. The first reflectance structure observed in other compounds of this sequence is a doublet attributed to spin-orbit transitions at the L point.[33,34] The energies of these transitions extrapolate somewhat below the doublet in CuI. The temperature shifts of the two minima are both ~ -0.4 meV/K, which suggests that both minima originate from the same location in the Brillouin zone. The spin-orbit splitting at the L point should be about two-thirds of the splitting at Γ. For CuI, Cardona has measured a splitting of 0.42 eV at the L point of the zone. Our observed splitting is only 0.20 eV.

However, according to photoemission measurements, the mixing at the edge of the zone is 23% iodine p electrons and 77% Cu d electrons. Using the rule[28]

$$\Delta_L = \tfrac{2}{3}[1.5(\xi_{Cu}\Delta_{Cu} + \xi_1\Delta_1)],$$

with -0.11 eV for the Cu d splitting and 0.95 for the I p splitting, this gives a splitting of 0.13 eV, which is close to our observed value. We therefore assign the peaks at 4.92 and 5.12 to a spin-orbit doublet along Λ near the L point.

Lewonczuk *et al.*[22] suggest that this peak is a result of normally forbidden transitions from the Γ_{12} valence band to the Γ_1 of the first conduction band, in agreement with their band-structure calculations. They argue, on the basis of the polarization dependence of this peak, that the symmetry requirements are relaxed due to strain. However, the Γ_{12} and Γ_1 regions are due to Cu $3d$ and Cu $4s$ electrons, respectively. Thus the oscillator strengths should be quite small. The observed strain dependence does not rule out our assignment, since such dependence has been observed[28] for the E_1, $E_1+\Delta_1$ transitions (Λ_3-Λ_1) of Ge and GaAs.

The next prominent structure in the thermoreflectance is a triplet extending from 6.0 to 6.6 eV and can be associated with three structures in the reflectance spectrum. This was previously

TABLE I. Interband-transition energies of the cuprous halides, obtained from thermoreflectance data at 85 K. Data for other compounds of the isoelectronic sequences are reproduced from Ref. 36. All energies are in eV.

Sample	C value[a]	E_1	E_2	$E_2+\delta$	E_1'	$E_1'+\delta$
Ge	0	2.42; 2.22[b]	4.44	5.6	5.86	6.04
Si	0	3.6[b]	4.43	5.46	5.95	6.7
Sn	0	1.36; 1.84[b]	3.6	4.1; 4.3	4.9	5.4
GaAs	2.9	3.02; 3.2[b]	5.03	5.9	6.62	6.9
GaP	3.3	3.8[b]	5.31	6.44	6.74	7.6
InAs	2.7	2.61; 2.88[b]	4.72	5.3; 5.5	6.25	6.74
ZnSe	5.6	4.75; 5.05[c]	6.7	7.20	8.30; 8.45	8.95; 9.20
ZnTe	4.5	3.58; 3.99[c]	5.37	5.95; 6.25	6.82	7.47
ZnS	6.2	5.7[d]	7.0	7.5	8.35	9.0
CuCl	8.3		6.8	7.4	8.3	10.0
CuBr	6.9	5.3	6.39	7.3	7.8	9.0
CuI	5.5	4.92; 5.12	6.12	6.36; 6.64	7.64	7.9
Region of BZ		$[L, \Lambda]$		$[X, \Delta]$		$[L, \Lambda]$

[a] Reference 2.
[b] Reference 34.
[c] Reference 33.
[d] F. H. Pollak, in *Proceedings of the International Conference on II-VI Semiconducting Compounds*, 1967, edited by D. G. Thomas (Benjamin, New York, 1968), p. 552.

assigned[6,26] to spin-orbit-split transitions from the top valence band to the second conduction band $\Gamma_{15}^{v_1}-\Gamma_{15}^{c_2}$ (for which, according to group theory) there should be three allowed transitions. The three minima have similar characteristics, which would be consistent with their originating from the same part of the Brillouin zone. They have a linewidth of ≈0.15 eV and a temperature shift of −0.5 eV/K. Cardona's[6] original interpretation, extrapolations from other compounds of the Ge-Sn, InAs, ZnTe, and CuI sequence, Van Vechten's[2] predictions, and the magnitude of the observed splitting were consistent with this assignment. As was pointed out, such a triplet structure has been previously observed[35] in GaAs. However, the E_0' structure observed by Cardona has been reinterpreted at least twice and the data used in the isoelectronic sequence extrapolation have been reinterpreted as well. For instance, in recent thermoreflectance measurements by Guzzetti *et al.*,[36] structure in ZnTe at 4.95 eV was labeled E_0' and was used in the previous extrapolation. However, these authors neglect to discuss the placement of this transition in the Brillouin zone and further this energy corresponds to $\Delta(8-10)$ $(0.5,0,0)$ transitions[37] according to previous band-structure calculations.[33] $E_0'(\Gamma_{15}^{v_1}-\Gamma_{15}^{c_2})$ transitions have been identified[34] with fair certainty in Ge-Sn and InAs. No structure in ZnTe is attributed to $E_0'(\Gamma_{15}^{v_1}-\Gamma_{15}^{c_2})$ but from the calculations the critical point energies are 5.8, 6.0, and 6.8 eV for the three components of the triplet.[33] These energies extrapolate out from 7.3 to 8.0 eV for CuI, hence other interpretations should be considered for the CuI triplet.

Lewonczuk *et al.*[22] proposed $X_1^{v_1}$, $X_5^{v_1}\rightarrow X_3^c$ transitions for this peak on the basis of their calculations for CuCl and CuBr. This is also consistent with the extrapolation from other compounds of the isoelectronic sequence, as indicated in Fig. 6. Hence we have reassigned this triplet to transitions from the three branches of the top valence band to the first conduction band at or near the X point. According to valence-band calculations by Goldmann *et al.*[14] the X_5-X_3 separation of the top valence band is about 0.6 eV. The higher-energy representation is doubly degenerate and

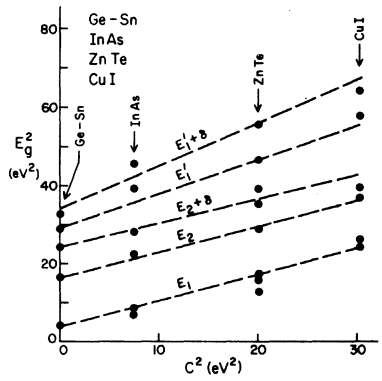

FIG. 6. Variation of energy gaps squared with the Phillips–Van Vechten ionicity parameter C squared for the CuI isoelectronic sequence. The C values were from Ref. 2.

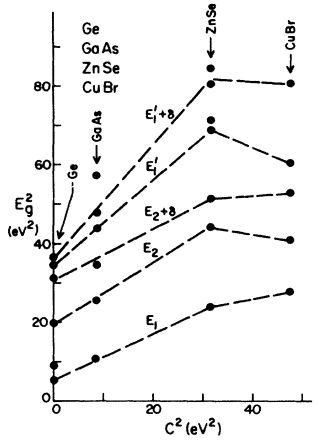

FIG. 7. Variation of energy gaps squared with the Phillips–Van Vechten ionicity parameter C squared for the CuBr isoelectronic sequence. The C values were taken from Ref. 2.

splits (X_6 and X_7) under the spin-orbit interaction. Our previous argument for the spin-orbit splitting at the L point, with appropriate change of sign in the equation, is applicable here, yielding an expected splitting of 0.3 for the X_5 representation. Since the X_5 representation of the first conduction band does not split, this yields expected splittings of 0.3 and 0.45 eV (assuming $X_5 \rightarrow X_5 + \frac{1}{2}\Delta$, $X_5 - \frac{1}{2}\Delta$). These values should be compared to the observed splittings of 0.24 and 0.28 eV between the lower and upper pairs, respectively, of the observed triplet.

Optical structure in the 6–7-eV region is also expected from the $\Gamma_{15}^{v_2} \rightarrow \Gamma_1^{c_1}$ transitions originating on the lower valence band at Γ, since the centroid of this band has been determined to fall 5 eV below the upper valence band maxima by x-ray-photoemission spectroscopy XPS measurements of Kono *et al.*[13] They conclude that for CuCl the lower valence band is predominately p-like in character so that a doublet, with a large splitting characteristic of the I ($5p$) is expected. In view of the strength of the first peak of the triplet, at 6.12 eV, $\Gamma_{15}^{v_2} \rightarrow \Gamma_1^{c_1}$ may contribute significantly to this structure with the second member contributing to the large broad reflectance peak beginning at 7 eV. Similarly, transitions originating on the second valence band at L and X, e.g., $L_1 \rightarrow L_1$ and $X_5 \rightarrow X_3$ probably contribute to the shoulder at 9 eV of the highest-energy reflectance peak. In spite of this overlap of transitions, we feel that the triplet near 6.0 eV contains significant contribution from first valence band transitions near X as indicated above.

Higher-energy thermoreflectance structure in CuI consists of two maxima at 7.64 and 7.90 eV. This doublet can be associated with a shoulder at 7.65 eV and a peak at 8.04 eV in the reflectance. It is likely that these two structures have different origins in the Brillouin zone since they have different temperature coefficients. There is no discernible shift for the lower-energy peak, while the higher-energy peak has a temperature coefficient of -7×10^{-4} eV/K. Similar differences are observed between the temperature coefficients of the E_1' and $E_1'+\delta$ transitions of other compounds of this isoelectronic sequence.[36] The energies of these transitions also extrapolate fairly well to those of CuI.

In ZnTe the lower-energy peak is attributed to volume effects (7–12) and (8–11) from the region around (0.6, 0.4, 0.3) and the higher-energy peak is attributed to (6–12) and (5–12) transitions in the same region plus transitions[37] along Λ (6–13). These considerations should be extended to CuI. Lewonczuk *et al.*[22] proposed that the higher-energy structure is due to $L_1^{v_1} \rightarrow L_1^{c_2}$ on the basis of their calculations. Van Vechten's predicted value for E_1' is 8.25 eV.

CuBr

Cardona[6] has shown that the reflectance peak at 5.3 eV corresponds to the peak at 4.7 eV in CuI, thus this peak is assigned to $E_1\,\Lambda$ (8—10) transitions. This peak decreases in intensity from CuI to CuCl in both the reflectance and thermo-reflectance. The interpretation of Lewonczuk *et al.*[22] that this is associated with $\Gamma_{12}^{v_1} \rightarrow \Gamma_1^{c_1}$ does not seem to be supported by this observation. It is expected that the d character of the Γ_{12} valence band and the s character of the Γ_1 conduction band should remain constant for the three compounds. Thus their interpretation should result in peaks of equal intensities for the three compounds. On the other hand, the oscillator strengths for transitions near the L point are expected to decrease from CuI to CuCl since the d character of the top valence band increases from CuI to CuCl and the s character at L_1 of the first conduction band is expected to be large and constant.

The thermorefelctance structure associated with the minima at 6.39 eV is assigned to transitions along Δ near the X point. This structure is similar to that observed in CuI when the smaller spin-orbit splitting is considered. (The expected splitting of about 0.1 eV is comparable to the instrumental resolution.)

The temperature shifts of the two low-energy peaks are both -4×10^{-4} eV/K while there is no detectable shift for the 7.73-eV reflectance peak. For this reason its assignment to E_1' is plausible. The peak at 9.0 eV has a temperature coefficient similar to that of the low-energy peaks and is

assigned to $E_1' + \delta$. The doublet observed in other TR spectra with a splitting of 0.3 eV is consistent with transitions from the top valence to the second conduction band near the L point as suggested by Lewonczuk *et al.*[22]

CONCLUSIONS

High-resolution, low-temperature data on the interband transition energies of the cuprous halides derived from reflectance and thermoreflectance techniques were obtained. Considerably more fine structure was resolved in the low-temperature measurements than had been previously observed.

On the basis of the splittings and temperature shifts observed, structure was assigned to transitions at various locations in the Brillouin zone. These assignments, which are summarized in Table I, were correlated with the interband energy gaps of other zinc-blende compounds, using the Phillips–Van Vechten ionicity scale. The observed correlation for CuBr is poor, while that for CuI is fairly good for transitions above the fundamental gap. This suggests that the ionicity theory of Phillips and Van Vechten does not apply as well to CuBr as it does to CuI. The most reasonable explanation for this lack of correlation is that the increased admixture of Cu-3*d* electrons in the top valence band is not properly accounted for in the theory. An attractive alternate explanation is that transitions originating on the second valence band contribute significantly to the spectrum. As noted above such transitions at Γ, X, and L are expected in the range 6–10 eV; however, we were unable to arrive at a consistent assignment of these transitions based on our present data.

ACKNOWLEDGMENT

This work was supported by the National Science Foundation Grant No. DMR77-09954.

[1]J. C. Phillips, Rev. Mod. Phys. 42, 317 (1970).
[2]J. A. Van Vechten, Phys. Rev. 182, 891 (1969); 187, 1007 (1969).
[3]H. Fesefeldt, Z. Phys. 67, 37 (1931).
[4]E. G. Scheider and H. M. O'Brayn, Phys. Rev. 51, 293 (1937).
[5]F. Herman and D. S. McClure, Bull. Am. Phys. Soc. 5, 48 (1960).
[6]M. Cardona, Phys. Rev. 129, 69 (1963).
[7]K. Shindo, A. Morita, and H. Kamimura, J. Phys. Soc. Jpn. 20, 2054 (1965).
[8]K. S. Song, J. Phys. Chem. Solids 28, 2003 (1967).
[9]F. Herman, J. Electron. 1, 103 (1955).
[10]S. Sato, T. Ishii, I. Nagakura, O. Aita, S. Nakai, M. Yokota, K. Ichikawa, G. Matsuoka, S. Kono, and T. Sagawa, J. Phys. Soc. Jpn. 30, 459 (1971).
[11]I. Ishii, S. Sato, T. Matsukawa, and Y. Sakisaka, J. Phys. Soc. Jpn. 32, 1440 (1972).
[12]D. C. Frost, A. Ishitani, and C. A. McDowell, Mol. Phys. 24, 861 (1972).
[13]S. Kono, T. Ishii, T. Sagawa, and T. Kobayasi, Phys. Rev. Lett. 28, 1385 (1972); Phys. Rev. B 8, 795 (1973).
[14]A. Goldman, J. Tejeda, N. J. Shevchik, and M. Cardona, Phys. Rev. B 10, 4388 (1974).
[15]S. Sato, M. Watanabe, T. Sagawa, S. Kono, S. Suzuki, I. Nagakura, T. Ishii, and R. Kato, *Vacuum Ultraviolet Radiation Physics* (Pergamon, Hamburg, 1974), p. 486.
[16]M. A. Khan, Solid State Commun. 11, 587 (1972).
[17]M. A. Khan, *"Molecular Spectroscopy of Dense Phases,"* in *Proceedings of XII European Conference on Molecular Spectroscopy* (Elsevier, Amsterdam, 1976), p. 89.
[18]E. Calabrese and W. B. Fowler, Phys. Status Solidi B56, 621 (1973); 57, 135 (1973).
[19]M. A. Khan, J. Phys. (Paris) 34, 597 (1973).
[20]R. S. Bauer, S. F. Lin, and W. E. Spicer, Phys. Rev. B 14, 4527 (1976).
[21]S. F. Lin, W. E. Spicer, and R. S. Bauer, Phys. Rev. B 14, 4551 (1976).
[22]S. Lewonczuk, J. G. Gross, M. A. Khan, and J. Ringeissen, Phys. Status Solidi B83, 161 (1977).
[23]J. Ringeissen, M. A. Khan, S. Lewonczuk, J. B. Gross, in Fifth International Conference on Vacuum Ultraviolet Radiation Physics, Montpellier, France, September 5, 1977 (unpublished).
[24]J. B. Anthony, A. D. Brothers, and D. W. Lynch, Phys. Rev. B 5, 3189 (1972).
[25]A. Zunger and M. L. Cohen, Phys. Rev. B 20, 1189 (1979).
[26]P. D. Martzen and W. C. Walker, Solid State Commun. 28, 171 (1978).
[27]J. G. Gross, S. Lewonczuk, M. A. Khan, and J. Ringeissen (unpublished).
[28]M. Cardona, in *Solid State Physics*, edited by F. Seitz, D. Turnbull, and H. Ehrenreich, Suppl. 11 (Academic, New York, 1969).
[29]B. Batz, in *Semiconductors and Semimetals*, edited by R. K. Willardson and A. C. Bier, (Academic, New York, 1972), Vol. 9.
[30]D. M. Roessler, Brit. J. Appl. Phys. 16, 1119 (1965).
[31]These samples were grown by Dr. C. Schwab, Universite Louis Pasteur, Strasbourg, France.
[32]Apache Chemicals Inc., P. O. Box 126, Seward, Ill., 61077.
[33]J. P. Walter, M. L. Cohen, Y. Petroff, and M. Balkanski, Phys. Rev. B 1, 2661 (1970).
[34]J. R. Chelikowsky, Ph. D. Thesis, University of Calif., Berkeley, Calif., 1975 (unpublished).
[35]D. E. Aspnes and A. A. Studna, Phys. Rev. B 7, 4605 (1973).
[36]G. Guizzetti, L. Nosenzo, E. Reguzzoni, and G. Samoggia, Phys. Rev. B 9, 640 (1974).
[37]In this notation, the bands are numbered consecutively,

with the highest-energy valence band numbered 8. The bands are doubly degenerate in the Δ and Λ directions, except for an extremely small splitting at L_4, L_5. Accordingly, a label (8–10) in one of these directions also includes transitions (7–9), (7–10), and (8–9). The proper group notation is used only where such labeling is unambiguous.